Fizika Nizkikh Temperatur, 1996, v. 22, No 3, p. 252–266

The role of quantized energy levels in the macroscopic quantum behavior of Josephson junstions

P. Silvestrini, B. Ruggiero, and A. Esposito

Istituto di Cibernetica del Consiglio Nazionale delle Ricerche, I-80072 Arco Felice, Naples, Italy

Submitted October, 25, 1995

The effects of the presence of quantized levels in the problem of the ($V = 0$)-state decay in Josephson junctions have been investigated. In considering the dynamics of the junction in the quantum picture, a preliminary study of the classical thermal fluctuation is necessary especially for the determination of the relevant junction parameters to be used in the quantum limit. Measurements of the lifetime of the zero-voltage state in a single hysteretic Josephson junction show clear evidence of two different damping regimes. Results are obtained for a wide range of damping within the underdamped region because the damping resistance depends exponentially on inverse temperature as does the junction quasiparticle resistance. This latter aspect is relevant because or allows to obtain a damping level that decreases with temperature, and hence, at low temperature we are able to study an extremely underdamped system. Many new interesting aspects related to the quantum behavior of the junction can be observed with such a low damping level. It is shown that a fast sweep of a Josephson tunnel junction can reveal the presence of quantum energy levels in the associated washboard potential. Peculiar effects, which can be observed on $P(I)$ and $\Gamma(I)$, are obtained by numerical integration of the entire time dependent master equation describing the dynamics of the statistical population of each quantum level. The curves obtained predict the results of possible new experiments. Finally, we discuss, within the well-established quantum picture of the junction, the idea of a resonant macroscopic quantum tunneling between levels with the same energy in neighboring wells of the potential shape describing the junction. This process produces small voltage spikes in the current-voltage characteristics, as well as peculiar peaks in the current switching distributions at given current values, which can be measured in junctions and SQUIDs with suitable parameters.

Introduction

In recent years great attention has been devoted to the study of the quantum behavior of a macroscopic system. Josephson devices are the most promising candidates for experimental investigation of the phenomenon. The quantum behavior of the Josephson phase leads to a host of interesting phenomena, including macroscopic quantum tunneling (MQT) [1], energy level quantization (ELQ) [2], macroscopic quantum coherence of two states (MQC) [1,3] and many states (Bloch oscillations) [4], and the Coulomb blockade of Cooper pair tunneling [5]. Macroscopic quantum tunneling (MQT) has been the phenomenon that first attracted the attention of the investigators, both from a theoretical and experimental point of view. Experiments on current-biased Josephson tunnel junctions with microwave irradiation support the idea of the existence of both MQT and ELQ [6–9], and the data are in good agreement with the theory [1,2,10]. In these experiments, one measures the decay probability of the supercurrent state of a Josephson tunnel junction and compares the data with the theory. At low temperatures, the contribution to the escape rate due to the quantum effects should be dominant over the classical thermal activation and therefore experimental subject to investigation. Very recently, an important experimental results [11], although referring to a SQUID rather than a single junction structure, clearly showed the occurrence of resonant macroscopic quantum tunneling (RMQT) in a macroscopic system.

The dynamics of a Josephson junction is described by a macroscopic quantum variable, namely, the phase difference φ of order parameters of superconductors on the two sides of the barrier. This variable is coupled to microscopic degrees of freedom, the quasiparticle excitations, and this circumstance produces dissipation in the system. In fact, the role of dissipation in the quantum behavior is one of the most stimulating implications in the phenomenon. There are several excellent theoretical works on the subject [1]. A complete theory of the phenomenon in Josephson tunnel junctions, taking into account all aspects of the problem in its full complexity, is, however, too complicated. One must then resort to simplified models which, within some reasonable approximations, allow us to obtain rather simple expressions for the escape rate useful for comparison with the data. The model widely used to fit data of this kind of experiments is the resistivly shunted junction (RSJ) model [12]. This model describes the junction in terms of a simple current biased lumped circuit consisting of a «Josephson» nonlinear element in parallel with a resistor R, which accounts for the junction dissipation, and a capacitor C, which accounts for the distributed capacitance of the structure forming the junction. The equations describing the junction dynamics within

© P. Silvestrini, B. Ruggiero, and A. Esposito, 1996

this model are identical to those of a mechanical analogue, consisting of a particle performing its motion in a washboard potential with a friction coefficient $\eta = \hbar^2/Re^2$. The relatively simplicity of the model allows us to take on the great complications coming from the introduction in the theory of the thermal fluctuations and of the quantum description of the junction. Within the framework of this model the computation techniques provide forms of the quantum escape probability out of the metastable state that are rather simply expressed in terms of relevant parameters of the junction, namely the critical current, the plasma frequency and the damping constant [1,2].

In the experiments, some of these physical quantities cannot be independently measured, and must be obtained from the experimental data as fitting parameters. However, the «large» number of free parameters and their mutual interdependence renders the best fit procedure quite delicate and uncertain. In fact at the present, the main difficulties in understanding the experiments lie in the extraction of the junction parameters from experimental data in order to allow a comparison with the theory.

In applying to Josephson junctions the results of the quantum calculations performed on the mechanical analog, one must also remember the strong approximations contained in the RSJ model. The weakest assumption of the model is the description of the strongly nonlinear junction dissipation simply by an ohmic resistance R. The results of the RSJ model are, however, used to fit the experimental data by implicitly assuming that one «effective» ohmic resistance can be considered fully responsible for the junction dissipation in the particular process considered. However, this resistance is not simply defined, since the current-voltage (I-V) characteristic of the junction is highly nonlinear in the subgap region. Because of that, a somewhat arbitrary fitting resistance has been assumed in many experiments. This aspect has been a cause of ambiguities and the problem is still a subject of debate in the scientific community. The few experiments on the subject [6–9,13–15], regarded as a whole, do not provide an unique answer for what concerns this effective resistance which should play an important role in the damping of the system. Rather, different authors reach contradicting conclusions about the value of resistance which fits the data of the theory. This is a natural consequence of the fact that the main limits of the RSJ model are, necessarily, included in this arbitrary fitting resistance. Moreover, one can also adjust the theory to the data with another free parameter which necessarily must be extracted from the data, i.e., the critical current. The use of free fitting parameters makes a quantitative agreement of data with the theory much easier, but the limits of the model may come out in the form of a subtle inconsistency of the fitting parameters [16]. Large discrepancies among different experiments are suspicious as long as they are not explained within a single coherent theory. Additional work, on both theoretical and experimental side, is needed to understand what is the actual significance which can be inferred from the data and what is the role of the damping in the macroscopic quantum decay.

In the present paper we review our recent results concerning some aspects of metastability of the zero-voltage state in hysteretical Josephson junctions. In considering the dynamics of the junction in the quantum picture, a preliminary study of the classical thermal fluctuation is necessary, especially for the determination of the junction relevant parameters to be used in the quantum limit.

Restricting ourselves to the thermal limit, we present a systematic attempt to give an answer to the still open question as to whether a single ohmic resistor can correctly describe the junction dissipation and what is this effective resistance. An experimental investigation in the thermal regime is surely useful to this purpose. We have performed measurements of switching current distributions in hysteretical Josephson junctions [13] and we have been able to investigate both the Kramers moderate damping regime and the extremely underdamped one [17,18]. From a theoretical point of view we have proposed an extended RSJ model, including in the equivalent circuit model the interference $\cos\varphi$ term as well as the possibility of a voltage-dependent resistance [15]. The theoretical results can be then compared with our data without free fitting parameters [19,20]. The good agreement between data and theory confirms the essential correctness of our assumptions, as well as the idea that, in our experimental setup, the dissipation is clearly dominated by intrinsic mechanisms due to the presence of thermally activated quasi-particles. This latter aspect is relevant because it allows us to obtain a damping level that decreases with the temperature, and hence, at low temperature we are able to study an extremely underdamped system.

Many new interesting aspects related to the quantum behavior of a junction can be observed with such a low damping level.

We now give an insight upon the effects of the presence of quantized energy levels in the supercurrent decay. We investigate the master equation developed by Larkin and Ovchinnikov [2] in its full time dependence. Many interesting features appear in nonstationary conditions [21,22], namely, when the escape process significantly reduces the statistical population of the metastable state and, as a consequence, the occupancy probability of the energy levels is far from the equilibrium. The effects of ELQ is in this case very relevant without the need of external microwave irradiation, and can be achieved by a suitable choice of the working parameters, such as sweeping rate and effective dissipation. Due to the presence of energy levels, the escape rate is an oscillating function of the bias current and the oscillation amplitude increases as the viscosity decreases, the effects being greater when the temperature T is higher than the crossover temperature T_0 [22]. The curves obtained predict the results of new possible experiments.

Finally, we discuss, within the well-established quantum picture of the junction, the idea of a resonant macroscopic quantum tunneling between levels with the same energy in neighboring wells of the potential shape describing the junction [23–27]. This process produces small voltage spikes in the current-voltage characteristics, as well as peculiar peaks in the current switching distributions at given current values, which can be measured in junctions and SQUIDs [11] with suitable parameters.

Effective junction damping

In this part, we discuss some implications of dissipation in the supercurrent decay, restricting ourselves to the classical thermal activation mechanism. The dissipative element is, in the real junction, due to the combination of different, non-linear mechanisms. At first glance, we can distinguish between intrinsic mechanisms of dissipation, related to the presence of quasiparticles excitations, and influences of the external circuit biasing the junction. Obviously, this latter aspect depends strongly on the experimental configuration, and, in some experimental situation, the junction dissipation may be dominated by any external resistive shunt [6] or load line [7–9].

Under some experimental conditions the external impedance loading the junction can play a fundamental role. In a resonant activation experiment [8], the authors have found that a good fit of the data is obtained with a value of resistance consistent with the estimated value determined entirely by the dissipation in the external circuitry. The results of this experiment have been then taken as «in situ» determination of system damping and interpreted in terms of the quantum regime [9].

Actually, measurements of the current switching distributions in the thermal regime [13] have shown that, in some experimental situations, the effective damping is dominated by an intrinsic resistance due to the presence of quasiparticle excitations. In view of many applications, it is desirable to have the system damping dominated by intrinsic mechanisms which set the lower limit for the junction dissipation [14]. In this case the voltage and phase dependence of the dissipation is particularly relevant [15].

Our analysis has been devoted to the probing of this important aspect [13,15,19]. We have studied the effect of a voltage-dependent junction resistance R_j on the critical current decay of Josephson junctions and have obtained a simple expression for the lifetime which takes into account the non-linear dependence of R_j on the voltage and on the phase, whatever it is [15]. This allows us to study the important case of dissipation completely dominated by the quasiparticle tunneling resistance. In this case it is, in fact, possible to obtain an analytical expression for the lifetime of the supercurrent state that can be compared with the experiments [15]. In fact, the effective resistance $R_{\rm eff}$ for the junction is related to a subgap resistance R^* by [15]

$$R^*/R_{\rm eff} = \left(1 + \sqrt{1+\alpha^2}\right)\left[\ln\left(\frac{b}{\sqrt{E_1}}\right) + \delta\right], \quad (1)$$

where $\alpha = I/I_c$, $b = \sqrt{2}e\mu/\hbar\omega_J$, $\delta = 0.2$, $\mu = \min(k_B T/e, \Delta)$, ω_J is the plasma frequency, and the value of E_1 is implicitly defined by the relationship [15]:

$$\ln(\sqrt{b/E_1}) + \delta = 1/\gamma E_1 \quad (\gamma = \Phi_0 I_c/(\pi k_B T)) .$$

R^* is defined as

$$R^* = \frac{4R_N k_B T}{e\Delta}\cosh^2\left[\frac{e\Delta}{2k_B T}\right]$$

where R_N is the junction normal resistance, $e\Delta$ and $k_B T$ are the energy gap and the thermal energy, respectively. Note that R^* can be interpreted as the resistance measured on the quasiparticle branch of the I-V characteristics at the temperature dependent voltage $V^* = \mu/n_e$ (n_e is the Naperian number, $V^* \ll \Delta$).

It is worth noting that the Eq. (1) can be used for comparison with experimental data.

The important parameters in comparing experiments and theory are the Josephson critical current I_c, the effective resistance $R_{\rm eff}$ and the effective temperature $T = T_{\rm bath} + T_N$. The former is a theoretical, unobservable, upper limit value of the randomly distributed observed values of the switching currents. Its direct measurement is impossible. The second one, $R_{\rm eff}$, is the parameter that we wish to determine from the experiments to compare with our theoretical value Eq. (1). Finally, the effective temperature T is equal to the measured quantity $T_{\rm bath}$ only in the ideal case where no external noise is present.

At first glance, a determination of the effective resistance can be obtained by fitting the data on the current switching distributions, leaving the effective resistance $R_{\rm eff}$ as a free parameter [13]. This procedure is correct as long as we are dealing with an extremely underdamped junction. The dissipation in our system is temperature dependent, therefore, the determination of the effective dissipation can be done only at temperature low enough that the extremely low damping regime has been reached [17,18]. In

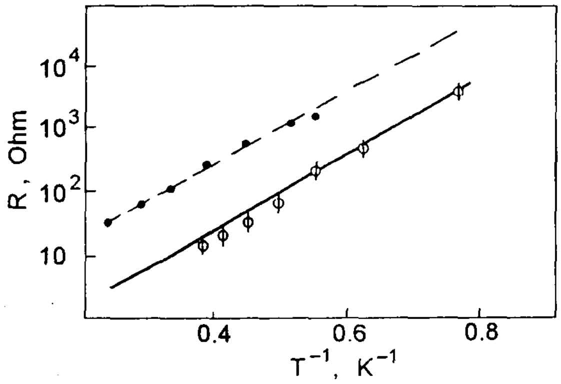

Fig. 1. Junction resistance vs. the reciprocal temperature on $Nb/NbO_x/Pb$ tunnel junctions. The dots are the resistances R^* measured on the I-V characteristic and the dashed line is the expected behavior with $\Delta = 1.3$ mV. The open circles are the effective resistance values R_{eff} as obtained from data on the switching current distributions and solid line is the expected behavior within our model.

Fig. 1, we report the values of the effective resistance (open circles) obtained by the fitting of the switching current distributions as a function of the reciprocal temperature [19]. The rather large error bars are due to the correlation with the other free fitting parameters. In order to get a useful quantity for the comparison we have also measured the subgap resistance $R^* = I^*/V^*$ on the dc current-voltage characteristics at the voltage $V^* = \mu/en_e$ (this voltage ranges between 75 and 120 μV for the considered temperature range 1.3–4.2 K). These values (dots) are reported in the Figure together with its expected theoretical behavior with $\Delta = 1.3$ mV (the dashed line). From the R^* values the effective resistance obtained within our model by Eq. (1) is shown as solid line. The very good agreement between data and theory confirms the fact that the junction dissipation is, in fact, dominated by intrinsic quasiparticle mechanisms. Moreover, since the friction parameter is strongly temperature dependent, we have investigated a very wide range of damping values just by changing the temperature.

In conclusion, a comparison of theory with experiments has been made by measuring the statistical distributions of the switching current in highly hysteretical Josephson junctions [13], which are related to the lifetime of the $V = 0$ state. The fitting of the data leaving R_{eff} as a free parameter allows to get informations about the effective dissipation. We have taken data in Nb–NbO_x–Pb Josephson junctions which pretty well agree with the theory, assuming that the junction resistance is due to intrinsic mechanisms of dissipation.

As a further consideration, we must point out that the high values of resistance obtained at low temperatures allowed us to study extremely underdamped systems characterized by the condition $\omega RC \ll 1$. In addition the intrinsic interest of this aspect in the thermal limit, this event opens new important possibilities to study experimentally macroscopic quantum effects. We will present our proposal in the next part.

Quantum picture

At the present, the observed quantum effects in experiments consist in either a «saturation» at low temperatures of the measured switching current distributions due to MQT (observed both in single junctions [6–9] and in SQUIDs [7]), and in a slight oscillating behavior of the $P(I)$ at microwave irradiation [9], due to the presence of quantized energy levels. Other experiments using very small Josephson junctions have been interpreted in the framework of the Bloch oscillation theory [4], but the actual significance of the phenomenon is still a matter of debate [30]. The damping value and the plasma frequency determine the temperature at which the quantum effects occur. However, it is difficult to distinguish the occurence of MQT from saturations due to some spurious experimental situations.

In fact, it may be possible by means of a suitable choice of the fitting junction parameters (namely those which cannot be known a priori), obtain a curve that fits the experimental data within the MQT theory, whatever the effective cause of the observed saturation [16].

The effect of the energy quantization is actually a peculiarity of quantum effects, producing an unambiguous oscillating behavior of the switching current distributions. An experiment, using microwave irradiation, has in fact given some evidence of the actual presence of energy quantizated levels in the junction [9]. The RMQT experiment lead on SQUIDs systems also shows evidence of energy levels in macroscopic systems [11]. In the following we show that a fast sweep of the current biasing the junction allows to obtain a clear evidence of the level discreteness, leading to nonequilibrium conditions in the well. This situations is characterized by the circumstance that escape process can induce an occupancy probability of the energy levels far from the equilibrium one. Our proposal does not require neither irradiation on the junction nor very low temperature. Moreover, the expected oscillation amplitude of the $P(I)$ is much larger of the one observed in Ref. 9, and it should allow a complete general study of quantum effects in the presence of dissipation.

In the quantum picture, we must consider the presence of energy levels in the potential well of the washboard potential associated to a Josephson tunnel junction. In the weak friction limit, there are, in fact, sharp and well separated energy levels inside the potential well, and the dynamic of the system can be described by the kinetic equation for the probabilities ρ_j of finding the particle at the jth level [2,21]

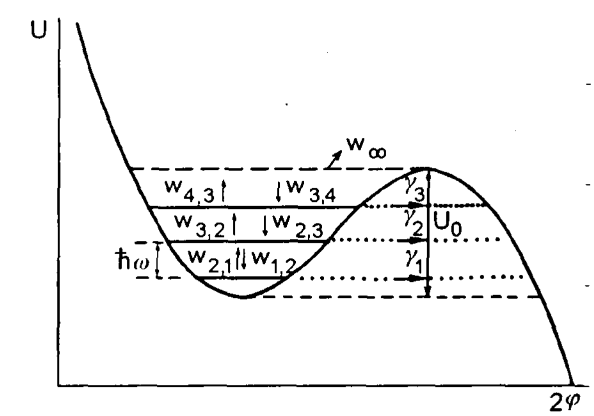

Fig. 2. Sketch of the dynamics inside the well in the presence of energy levels.

$$\frac{\partial \rho_j}{\partial t} = \sum_k (w_{jk}\rho_k - w_{kj}\rho_j) - \gamma_j \rho_j , \qquad (2)$$

where w_{jk} is the probability for transition from the kth into the jth level due to the interaction with the heat bath, and γ_j is the probability of tunneling through the barrier which strongly depends on the energy level position E_j. A sketch of the dynamics is shown in the Fig. 2.

We notice that most of the works on the subject refer to the stationary case, whereas in order to obtain a complete description of the quantum behavior of a macroscopic variable, a correct understanding of the non-stationary case is also necessary [21,22,31].

The present analysis is, in a sense, complementary to that by Kopietz and Chakravarty [31], who also find time-dependent solutions of the master equation at a fixed bias current for various initial distributions. However in our work, we focus the attention on the effect of the rate of change of potential barrier and the non-stationary conditions come out as a consequence of the fast sweep rate of the bias current. In fact, the effect of the ramp rate is here included and the curves obtained predict the results of new interesting experiments. The effects of the energy level quantization and of the tunnel probability on the escape rate out of a metastable state in non-stationary conditions is enhanced at temperatures much larger than the crossover temperature T_0. This peculiarity which respect to the usual stationary conditions renders the present aspect very interesting in view of the experiments.

The behavior predicted by Eq. (2) can be qualitatively understood by the following considerations. For sufficiently deep levels, the tunneling probability γ_j is typically small compared to the w_{jk} elements. Actually, the upper levels undergo a reduction due to the high escape rate values, γ_j, which, in turn, produce nonstationary conditions in the well. However, if the rate of change of the bias current is so slow that the shape of the potential does not change significantly during the typical relaxation time of the system (related to transition probability between levels), the process is adiabatic and we are quasi-stationary conditions. That is, at each value of current, there are many transitions between levels which are able to give rise to a thermal diffusion process from the lowest levels to the upper levels. This refills the upper levels, and a quasi-stationary distribution inside the well is reached. In this case $\Gamma(I)$ does not depend on rate of change of the bias current, dI/dt, and all the escape events will occur for high potential barriers and in presence of many energy levels (for typical Josephson junctions). The escape rate can then be calculated in the quasi-stationary approximation, looking for the steady state solutions of Eq. (2).

The nonstationary conditions come out as a consequence of a fast sweep of the junction bias. In fact, the potential barrier reduces with increase in the current. Hence, the total number N of levels in the well depends on I, and, as a consequence, on the time: $dN/dt = (dN/dI)(dI/dt)$. If the sweep rate is so fast that only few transitions between levels can occur during the time necessary for the last level to reach the top of the barrier, then the refilling from the lowest levels by thermal diffusion has not time to take place. After a certain number of switching events, related to the initial probability $\rho_N(0)$ of finding the upper level populated, there is a rapid decrease in $P(I)$ as the level is empty. In this case, $\Gamma(I)$ and $P(I)$ are oscillating functions of the current, with a period related to the level spacing. To describe this process in its nonequilibrium nature, one has to consider the dynamics described by Eq. (2) in its full time dependence. We have initially the particle in thermal equilibrium in a very deep potential well, corresponding to the initial current value $I_0 = I(t{=}0) \ll I_c$. We then have to follow the evolution with the time of the system accounting for the diffusion process inside the well, the escape probability and the rate of change of the potential due to the change of the bias current.

The positions of the levels, the transitions between levels and the tunneling probabilities will be calculated by expressions obtained in Ref. 2 considering the cubic approximation for the Josephson potential. The system is initially trapped in a relative minimum of the potential, but it can escape from the well via either macroscopic quantum tunneling or thermal activation. In this case a switching from the $V = 0$ to the $V \neq 0$ state is observed in the junction.

Experimentally the bias current is a periodic function of time, and the transitions from the $V = 0$ to the $V \neq 0$ state are repeatedly observed at random values of I smaller than I_c. The physical quantity directly measured is the distribution $P(I)$ of the current switching values. In statistical terms, we can say that the «total» probability of finding the particle inside one of the potential wells at the initial time is a certainty, $\rho(t{=}0) = 1$. However, there exists a certain probability of escape from the well leading to a $\rho(t)$ which is a decreasing function of time (obviously, since I is increasing with time at a certain sweep rate, ρ can be seen as a function of the current as well). It is easy to correlate the measured quantity $P(I)$ with $\rho(I)$:

$$P(I) = -\frac{d\rho}{dI}\,. \qquad (3)$$

Although the lifetime of the $V = 0$ state loses its classical meaning under nonstationary conditions, since it now depends not only on the current, but also on the initial condition as well as on the rate of change of the potential, it is, however, useful to define a «generalized» total escape rate $\Gamma(I)$, in analogy with the quasi-stationary case, as

$$\Gamma(I) = -\frac{d \lg [\rho(t)]}{dt} = -\frac{d \lg [\rho(I)]}{dI}\frac{dI}{dt}\,. \qquad (4)$$

At the initial time, the statistical populations of energy levels are distributed according to the Boltzmann distribution

$$\rho_j(0) = A \exp\left(-\frac{E_j}{k_B T}\right), \qquad (5)$$

where ρ_j is the population of the jth level or the probability to find there a particle. It is clear that $\rho(t) = \Sigma_j \rho_j$ and $\Sigma_j \rho_j(0) = 1$; $A = 1/\Sigma_j \exp(-E_j/(k_B T))$ is a normalization factor.

All the curves reported here are obtained by numerical solution of the master equation (2). It has been solved with the Boltzmann distribution Eq. (5) as initial condition, namely, the system is initially in thermal equilibrium in a very deep potential well corresponding to the initial current value $I_0 = I(t{=}0) < I_c$. Starting from this time we follow the time evolution of the levels population numerically, taking into account that the current is also changing with the time.

We present here simulated $P(I)$ and $\Gamma(I)$ curves at various temperatures, for some experimentally significant junction parameters, and for different values of the sweep rate dI/dt.

Effects of the ramp rate

The presence of quantized energy levels can be revealed by a fast sweep of the junction bias [21], which in turn produces a rapid change in the potential shape and a fast reduction of the potential barrier U_0. The effect can be summarized here by the following argument: during the escape process the population of the upper levels experiences a fast escape rate and this tends to push the system out of thermal equilibrium. If the sweep rate is so fast that the refilling from the lowest levels by thermal diffusion has not enough time to take place, the upper levels will be depopulated and once almost empty can no longer contribute to the escape. Hence, until the next level approaches energy values suitable for activation, there is a rapid decrease in the decay rate. This occurs periodically and leads, in the current switching distributions of the junction, to an oscillatory behavior which is a clear manifestation of the presence of quantized energy levels.

This considerations can be visualized in Fig. 3.

In the left column the switching current distributions are reported for various decreasing values of the sweep rate. In the right column the corresponding populations of the levels in the well are reported as a function of the bias current, in order to visualize the evolution of the level populations in the various cases. For the higher value of the sweep rate, the oscillatory behavior is clearly shown, with many minima of $P(I)$ related to the position of the levels. Looking at the corresponding evolution of the system, it is clear that the diffusion process from the lower levels does not occur, and the populations remain essentially constant, except for the level close to the barrier top, which undergoes a fast reduction due to the escape process. By reducing the rate of change of the potential barrier, the diffusion from the lower levels has more time to refill the upper level, and this tends to destroy the oscillatory behavior in the escape rate. At the lowest sweeping rate, the oscillatory behavior disappeared completely, corresponding to a large thermal diffusion from the bottom of the well, which kept a quasi-stationary situation in the well. Let us now give a look at some other features of this peculiar effect.

Temperature dependence of the quantum effects

The temperature dependence of the effect is shown in Fig. 4. In discussing the Figure, the bath temperature T must be compared with the cross-over temperature $T_0 = \hbar\omega_J/2\pi k_B$, which, in our simulation, is ranging between 100–140 mK, depending on the bias current. The first situation is shown at a temperature $T < T_0$ (T = 100 mK). In this case almost all the switching occur at currents values corresponding to the presence of only one level in the well. In fact, at low temperatures almost all the particles are initially in the ground state, the transition element w_{ij} between levels are small and there is no time to populate other levels when you run at fast speed. All the particles are «frozen» in the ground state, so that one cannot see the typical oscillations due to levels discreteness. These fluctuations are evident increasing the temperature, namely for $T > T_0$. They are more evident in the lower dissipation junction, because the

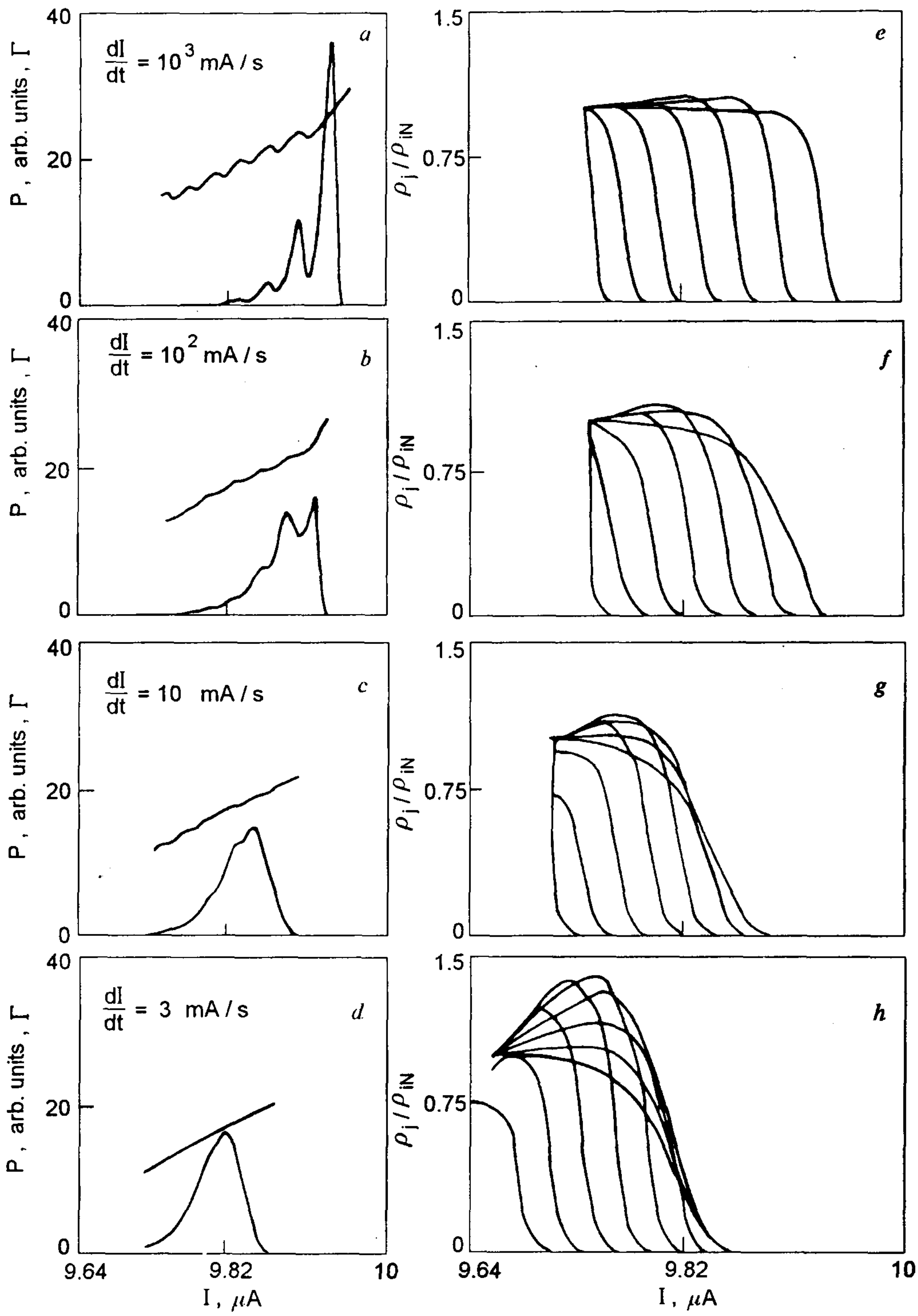

Fig. 3. Switching current distributions $P(I)$ and escape rates $\Gamma(I)$ (left column) and the corresponding levels population evolution (right column) reported as a function of the current I at various values of the bias frequency dI/dt, mA/s: 10^3 (*a*), 10^2 (*b*), 10 (*c*), 3 (*d*). The levels populations ρ_j are normalized to the initial Bolzmann population $\rho_{j0} = \rho_j(t=0)$, in order to have all of them in the same scale. The simulation is performed for the following junction parameters: $I_c = 10\,\mu$A; $C = 5$ pF; $R = 100$ kOhm; $T = 200$ mK.

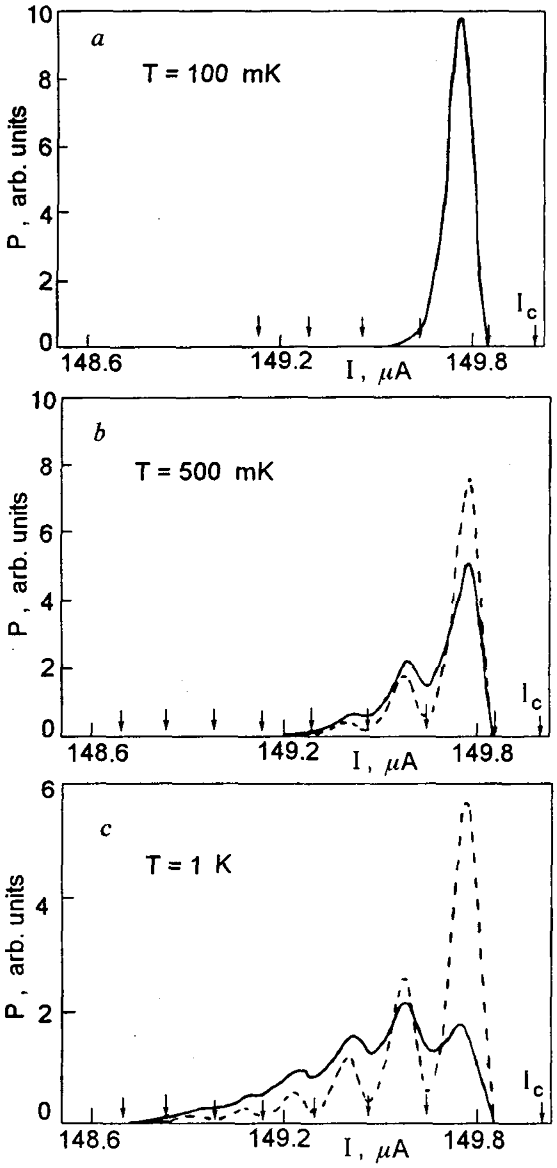

Fig. 4. Current switching distributions $P(I)$ vs. I as obtained by numerical integration. The simulated curves refer to a junction with $I_c = 150\,\mu$A and $C = 5$ pF. The sweep rate is here $dI/dt = 10^5$ mA/s. Two damping resistance values, $R = 1$ kOhm (solid lines) and $R = 100$ kOhm (dashed lines), have been considered at different temperatures T, mK: 100 (*a*); 500 (*b*); and 1000 (*c*). For this junction parameters the crossover temperature is $T_0 = 100$–140 mK in the considered bias range. The arrows indicate the current values for which an energy level approaches the too high energy barrier. Note that in the case *a*) (i.e. $T = 100$ mK), the dashed and solid lines are coinciding.

transitions probabilities between levels are smaller. Under this conditions the area under each peak is close to being proportional to the initial population of the corresponding level. Increasing the temperature we can observe a larger number of oscillations since the initial Bolzmann population is spread out over many levels. It is obvious that this is true only up to

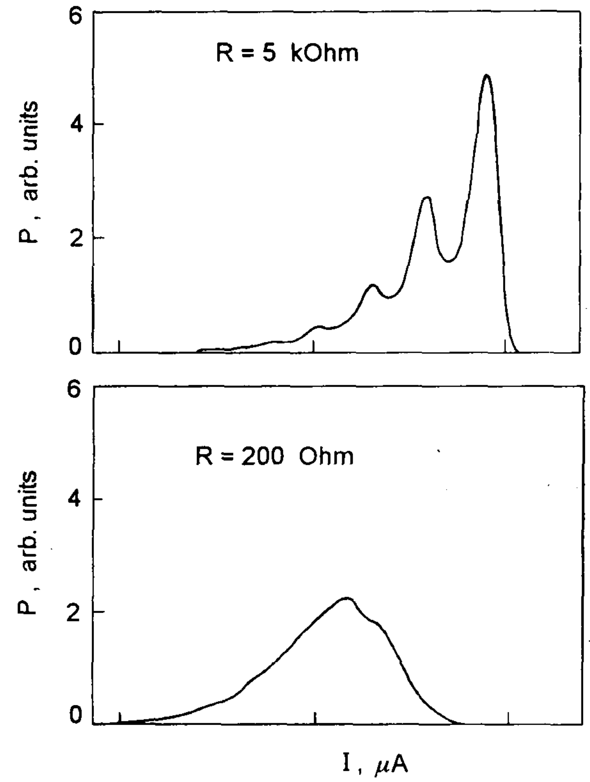

Fig. 5. Switching current distributions $P(I)$ at $T = 700$ mK, for two significant effective resistance values. Here $dI/dt = 3\cdot 10^4$ mA/s, $I_c = 150\,\mu$A and $C = 5$ pF.

values of T not so large as to permit many transitions between levels and, as a consequence, a repopulation of the upper levels. The upper limit for T to observe the oscillations due to the level discreteness depends on the damping level, which also influences the w_{ij} elements. The curves shown refer to a set of junction parameters which leads to a crossover temperature $T_0 = 100$ mK, but the analysis of the results allows us to extend the conclusions to different junction parameters with different T_0 values.

Dependence on the effective resistance

The effect of the damping level is shown in Fig. 5. In the higher resistance junction the oscillatory behavior is evident. The oscillation amplitude reduces as the resistance decreases; in fact, an increase in dissipation leads to higher transition probabilities between levels and to a faster thermalization. The diffusion from the lower levels is able to restore a quasi-equilibrium situation, which tends to destroy the oscillatory behavior. The curve for $R = 200$ Ohm does not present, in fact, any evident effects due to the energy levels discreteness.

Resonant macroscopic quantum tunneling

Current biased Josephson junctions

In this part we wish to discuss, within the well established quantum picture of the junction, the effect of the temperature on the resonant macroscopic quantum tunneling (RMQT) between levels with the same energy in neighboring wells of the potential shape describing the junction. This process produces sharp voltage peaks in the current-voltage (I-V) characteristics at given current values, which can be measured in junctions with suitable parameters, and characteristic peaks in the switching current distribution. The phenomenon has been already analyzed by different authors [23–27]. In Ref. 23, in particular, a detailed analysis of the resonant tunnel dynamics is presented for the $T = 0$ case, with a complete description of the experimental conditions for a check of the phenomenon. From this $T = 0$ analysis, it is clear that the lifetime of the voltage peaks has a relevant role for the observation of such steps. In fact, the lifetime decreases as the voltage amplitude increases. Recently, a different approach, which explicitly includes the temperature, has been discussed in Refs. 26, 27; although without including the lifetime of the resonant states.

We now extend the analysis of Ref. 23 and 26 studying the lifetime including the effect of temperature. In particular, were present the lifetime of the resonant voltage state at various temperatures as a function of the junction parameters. In view of experiments, this allows us to chose the junction parameters in order to maximize the merit factor $\chi = V\tau^{1/2}$, and to balance between measuring extremely small signals of longer duration or larger signals of shorter duration.

The system is initially trapped in a relative minimum of the washboard potential $U(\varphi)$, but it can escape from the well via either MQT or thermal activation. For values of the normalized current smaller than $\alpha_0 \approx 0.2$ the ground state in the first well will lie on an energy smaller than the upper level of the second well (Fig. 6).

In the following we restrict our analysis to the case of the ground state of one well lying at energy close to the first excited level in the next well. In this case the particle coming via MQT from the ground state will go into the first level and then can either decay or perform a successive tunneling. These competitive processes lead to different results. For each current value we must in fact define two possible junction states which produce different observable solutions: one is the «free running state» where the system after a series of successive tunneling is freely running down the potential slope with energy E larger than the barrier energy U_0 ($E > U_0$). This state is characterized by junction voltage corresponding to the quasi-particle branch of the I–V curve. In the other state, which we call «resonant state», the system performs a sequence of tunneling and decay processes, being trapped in one of the wells at a certain energy level ($E < U_0$). The resonant state is characterized by a junction voltage corresponding to the phase mobility due to the tunneling across the barrier. Assuming that tunneling from the ground state to the first excited state is the most relevant process, the average voltage will be $eV \approx \pi\hbar\gamma_0$. The tunnel probability γ_0 has the resonant behavior for current values for which the ground state corresponds to one of the excited states of the next well [25–27]. This produces a fast increase of the voltage at certain current values and voltage steps on the I–V curve. The probability ρ of finding the system in the resonant state is obviously $\rho = \Sigma_j \rho_j$, where ρ_j is the occupancy probability of the jth level. The junction dynamics is well described by the following kinetic equation:

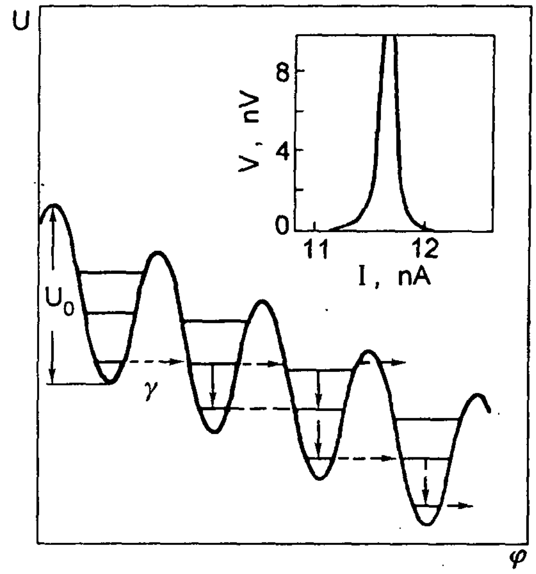

Fig. 6. Potential $U(\varphi)$ describing the junction dynamics. A sharp voltage peak in the I–V characteristics appears when the ground state lies on an energy level very close to one of the first excited states in the next well; this is shown in the inset for the following junction parameters: $E_0/\hbar\omega_j = 2.5$, $T = 50$ mK, $I_c = 200$ nA, and $R/R_Q = 100$, where $R_Q = \pi\hbar/2e^2 = 6.45$ KOhm.

$$\partial\rho_j / \partial t = \Sigma_k(w_{j,k}\rho_k - w_{k,j}\rho_j) - \gamma_j\rho_j + \gamma_{j-1}\rho_{j-1} \quad (6)$$

where $k = 0, ..., N$ (referring 0 to the ground state and N to the upper level in the well). Eq. (6) for resonant conditions differs from Eq. (2), valid for $I >> 0.2I_c$, because of the last term in the right side, which indicates that the particle tunneling from the $(j-1)$th level goes into the jth level in the next well. Following a rather standard procedure for quasi-stationary processes, we can now obtain a general expression for the lifetime of the resonant state. Assuming initially the junction in the resonant state, $\rho(t=0) = 1$, $\rho(t)$ tends to reduce with time due to an escape rate Γ to the free running state. The lifetime τ of the resonant state can be assumed as the reverse of Γ, $\tau = \Gamma^{-1}$. As usual, in quasi-stationary condition Γ is defined as

$$\Gamma = -(1/\rho)\,\partial\rho/\partial t \ . \qquad (7)$$

Summing the system of Eq. (6) over all j, the following expression for $\partial\rho/\partial t$ is obtained:

$$\partial\rho/\partial t = -(w_\infty + \gamma_N \rho_N) \ , \qquad (8)$$

where w_∞ is the transition probability to the continuum.

In quasi-stationary conditions ρ_N can be related to ρ by finding the steady-state solution of Eq. (6). By simple calculations we obtain

$$\rho = (1 + \Sigma_j A_j)\rho_N \ , \ j = 0, ..., N-1 \ , \qquad (9)$$

where

$$A_j = \Pi_k(w_{k,k+1} /(w_{k+1,k} + \gamma_k)) \ , \quad k = j, ..., N-1 \ . \qquad (10)$$

By definition (Eg. (7)) we obtain

$$\Gamma = (w_\infty + \gamma_N)/(1 + \Sigma_j A_j) \ , \quad j = 0, ..., N-1 \ . \qquad (11)$$

In this way we arrive at a general expression for Γ as a function of $w_{j,k}$ and γ_k, which depend strongly on the temperature T and junction parameters. At low temperature [$k_B T << \hbar\omega_j$, where

$$\omega_j^2 = (1 - \alpha^2)^{1/2}(2eI_c/\hbar C) \ ],$$

we can neglect the transition probability $w_{k+1,k}$ toward higher levels, hence, $w_{k,k+1}/w_{k+1,k} \approx \approx \exp[(E_{k+1} - E_k)/k_B T] >> 1$, and we also expect that $w_{k,k+1} >> \gamma_k$ (except very close to the resonant conditions). In this case Eq. (11) reduces to $\Gamma \approx \gamma_N /\Pi_k(w_{k,k+1}/\gamma_k)$ and therefore Γ decreases strongly with increase in the ratio $w_{k,k+1}/\gamma_k$. This corresponds to the trivial physical consideration that Γ is small when the competing decay probability is much larger than tunnel probability, the alteration of tunneling to the first level and decay down to the ground state being the most likely process.

For γ_0 close to the resonance we actually use the formula obtained by Larkin, Ovchinnikov, and Schmidt [32] calculated for $kT << \hbar\omega_j$:

$$\gamma_0 = A\omega_j \exp(2S + 1)[\omega_j/\delta\varepsilon(1 + \coth(\delta\varepsilon/2kT)) + + B/\omega_j(\omega_j/\delta\varepsilon)^2] \qquad (12)$$

here $A = 3\hbar^2/8Re^2$, $B = e^2/2\pi^2 C$, S is an action under the barrier, and $\delta\varepsilon$ is the energy difference referring to resonant energy levels in different wells. Equation (12) is valid only for large enough values of $\delta\varepsilon$, namely, when $\delta\varepsilon > \hbar^2\omega_j/(Re^2)$ [32]. As it is easy to see, the transition probability is an asymmetric function of the energy difference $\delta\varepsilon$. The results of the calculations at different temperatures are reported in Figs. 7–11.

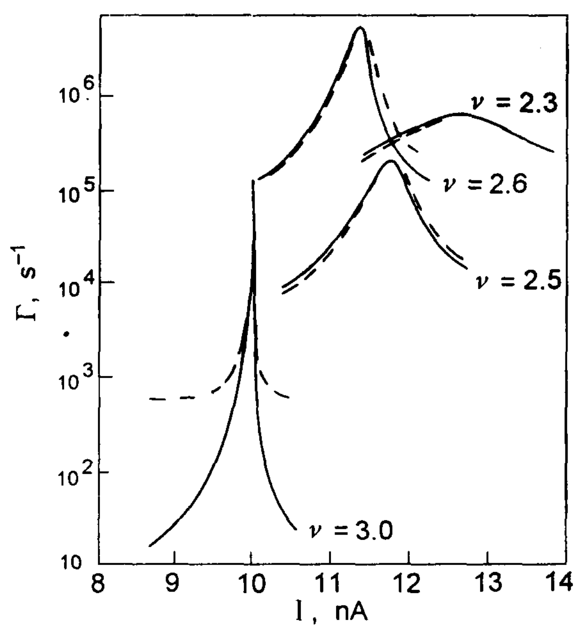

Fig. 7. Escape rate as a function of the current in the region of the resonance for different values of ν at $T = 50$ mK (solid lines) and $T = 200$ mK (dashed lines).

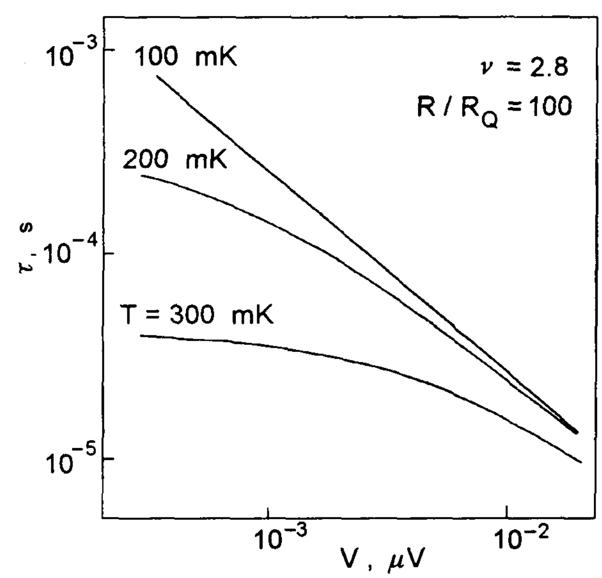

Fig. 8. Lifetime of the resonant state as a function of the voltage along the step, at different temperatures and for $\nu = 2.8$.

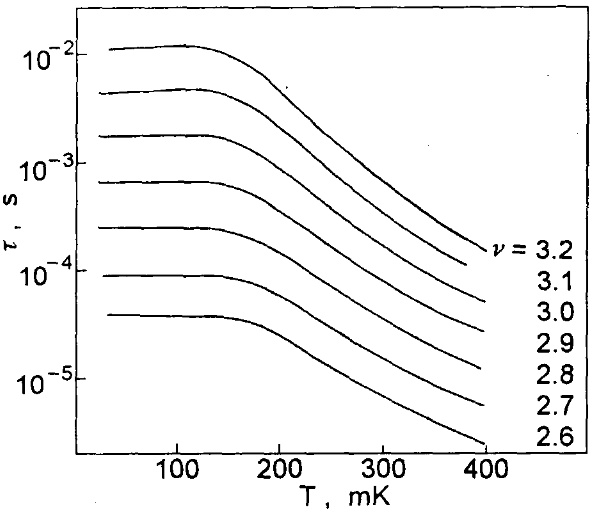

Fig. 9. Lifetime of the resonant state as a function of temperature, for different values of ν, at fixed voltage of the resonant state: $V = 1$ nV (for the considered ν values, 3 levels are present in the potential well).

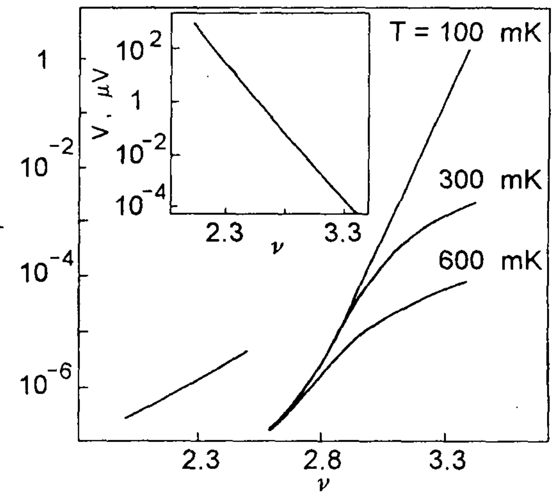

Fig. 11. Maximum voltage of the resonant state lifetime as a function of ν at various temperatures. In case of 2 levels in the well ($\nu < 2.5$) the curve is almost temperature independent. In the inset is shown the step voltage amplitude as a function of ν, the curve is independent of the temperature.

We consider different values of the ratio $E_J/\hbar\omega_j$, typically refered to as ν in literature [23]. This parameter can be also defined in terms of the ratio of the Josephson energy $E_J = \hbar I_c/2e$ and the charging energy $E_c = e^2/C$, $\nu = (2E_J/E_c)^{1/2}$. It is connected with the number of levels inside the well and it increases with increase in the capacitance. This dimensionless quantity is of the most importing accounting for the effect of the junction parameters. The values considered refer to junction capacitance ranging between 7–22 fF, and critical current $I_c = 200$ nA. The resistance value, which also strongly affects the results, has been fixed at $R = 645$ kOhm in order to satisfy the condition of validity for Eq. (12). Junctions with these parameters can be built by standard fabrication technique, although to obtain an effective impedance $R \gg R_Q = 6.45$ kOhm in any real experimental configuration a great care in insulating the junction from the external electronics and environment is required and it may present a difficulty [8].

In Fig. 7 we plot the escape rate as a function of the current for ν ranging between 2.3 and 3, and at different temperatures ($T = 50$ mK and 200 mK). As a general consideration, we note that the escape rate presents, for a current close to the resonance, a peak whose sharpness increases with increasing ν and with decrease in temperature. Γ ranges between $10-10^5\ \mathrm{s}^{-1}$ for $\nu = 3$ and $T = 50$ mK, whereas it is almost flat ($10^6\ \mathrm{s}^{-1}$) for $\nu = 2.3$ and $T = 200$ mK. The effect of temperature is larger for larger ν values, mostly because of different «quantum temperatures» $T_Q = \hbar\omega_j/k_B$, being $T_Q = 1.51$ K for $\nu = 3$ and $T_Q = 1.97$ K for $\nu = 2.3$. These Γ values could be quite accessible in measurements of the current switching distributions using the existing techniques [6–8,13].

In order to discuss the possibility of observing the RMQT voltage peaks on the supercurrent branch of the I–V characteristics, we consider the lifetime τ of the resonant state which can be defined as the reverse of Γ, $\tau = \Gamma^{-1}$.

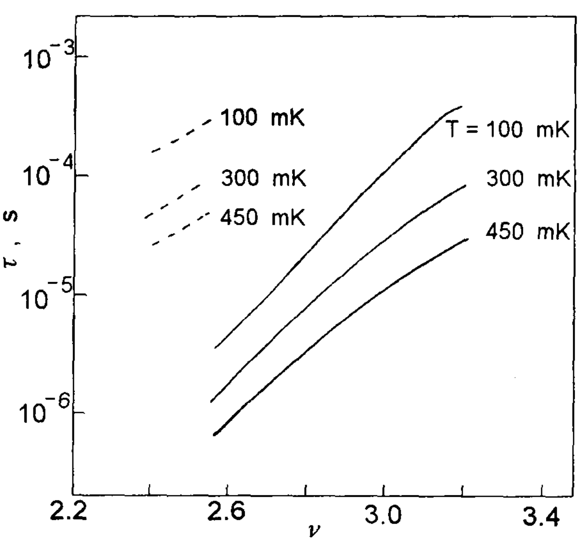

Fig. 10. Lifetime of the resonant state as a function of ν, for different values of temperature, at fixed voltage of the resonant state, $V = 3$ nV. The curves present a discontinuity at ν value for which the levels inside the well change from 2 (dashed lines) to 3 (solid lines).

In Fig. 8 we plot the lifetime τ as a function of the voltage along the step for $\nu = 2.8$ and at various temperatures. Considering a figure of merit $\chi = V\tau^{1/2}$, we find that χ ranges between $10^{-11}-10^{-10}$ V·Hz$^{-1/2}$, making a direct observation of the voltage peaks on the I–V curve a hard goal.

In Fig. 9, we show τ vs. T at a fixed step voltage on the I–V curve and different values of ν: $V = 1$ nV for $\nu = 2.6$–3.2 (three levels in the well). This temperature dependence shows an exponential behavior with saturation at low temperatures. A saturation temperature T_s can be identified for the whole family of curves. This temperature is related to the quantum temperature, roughly as $T_s = T_Q/10$. Although this temperature cannot be given by a precise value, due to its slight dependence on other junction parameters and voltage amplitude, it can provide an indication of the temperature range of experimental interest in choosing the actual working conditions.

In Fig. 10 we report the dependence of τ as function of ν at different temperatures. Here the step-voltage has been fixed at $V = 3$ nV. We note an exponential dependence with a strong discontinuity in changing the levels in the well from two to three. In fact, close to resonance, it is relatively easy to find the system in excited levels, and the escape rate is therefore dominated by the tunnel probability from the upper level, which strongly depends on its energy. The upper energy level is very close to the barrier energy when one more level can stay in the well.

Finally, we now want to consider the voltage amplitude calculated at a given energy difference between the resonant energy levels: $\delta\varepsilon = \hbar^2\omega_j/(Re^2)$. In Fig. 11 we report the corresponding lifetime of the resonant state at different temperatures. In the inset is shown the voltage step amplitude as function of ν.

We remark that our approach allows us to include the temperature in the calculations, both for what concerns the resonant tunnel probability, γ_0, and the escape rate to the free running state. Our results, extrapolated to $T = 0$, are in good agreement with those obtained in Ref. 23 by a different approach, confirming the great difficulties one would find in trying to detect the voltage steps. This is due to the small lifetime ($\tau \approx 0.1$–1 ms) for voltages large enough to be measured ($V \approx 1$ nV) in the low temperature range ($T < 200$ mK). The effect of RMQT on the switching current distributions seems at the moment the most readily observable effect. So far as the temperature behavior of the lifetime is concerned we found an exponential dependence with a saturation at low temperatures ($T < T_Q/10$).

RMQT in SQUIDs

Very recently, in an important experiment performed on a SQUID system Rouse, Han and Lukens reported the first observation of resonant tunneling (RMQT) between macroscopically distinct quantum levels [11]. The experiment consisted of varying the applied flux Φ_x linearly in time to tilt the potential at the rate of about 20 K/s, reducing the barrier of the upper level until a fluxoid transition occurs. The value of Φ_x for this transition is then recorded and the sign of $d\Phi_x/dt$ reversed, tilting the potential back until the system returns to the original well. This process is repeated approximately 10^4 times, generating a histogram of the transition probability $P(\Phi_x)$, which is then related to escape rate $\Gamma(\Phi_x)$. At low temperatures the escape rate $\Gamma(\Phi_x)$ between two different fluxoid wells vs. Φ_x exhibits a series of local maxima where the ground state of the upper well croses an excited state of the lower well.

The observed oscillation amplitude due to RMQT [11] is much larger than the slight oscillating behavior of Γ observed in single Josephson junctions [9] in the presence of microwave irradiation. Moreover, the positions of the maxima agree well with the calculated level crossing and therefore the experiment is unambigously interpreted as due to quantum effects, even without a precise comparison between data and theory.

A number of authors have predicted effects related to RMQT in current-biased Josephson junctions, but no specific analysis for SQUID systems has been reported in the literature so far. The rf SQUID is described by the following potential energy [11] $U(\Phi, \Phi_x) = U_s[(\Phi - \Phi_x)^2/2 + \beta_L \cos\Phi]$, where Φ and Φ_x are fluxes in units of $\Phi_0/2\pi$ measured with respect to $\Phi_0/2$, $U_s = \Phi_0^2/4\pi^2 L$, and $\beta_L = 2\pi L I_c/\Phi_0$ is a measure of the total critical current in terms of the current required to create Φ_0 in the loop. For $\Phi_x \neq 0$ this potential is symmetric double well with the left and right wells corresponding to the 0 and 1 fluxoid states of the SQUID, respectively. For $\Phi_x = 0$, the potential is tilted, resulting in an energy difference ε between the minima of the wells. As Φ_x is increased the barrier ΔU for the upper well decreases roughly linearly with ε [11]. In extending our theoretical calculations to rf SQUID systems we must take into account that a different observable state is reached after each tunneling event, while in a single current biased junction this is obtained only after a sequence of tunneling events. At low temperature, we can just consider the transition probabilities $W_{0,k}$ and $W_{0,k+1}$ from the ground state $E_0^{(\mathrm{up})}$ of the upper

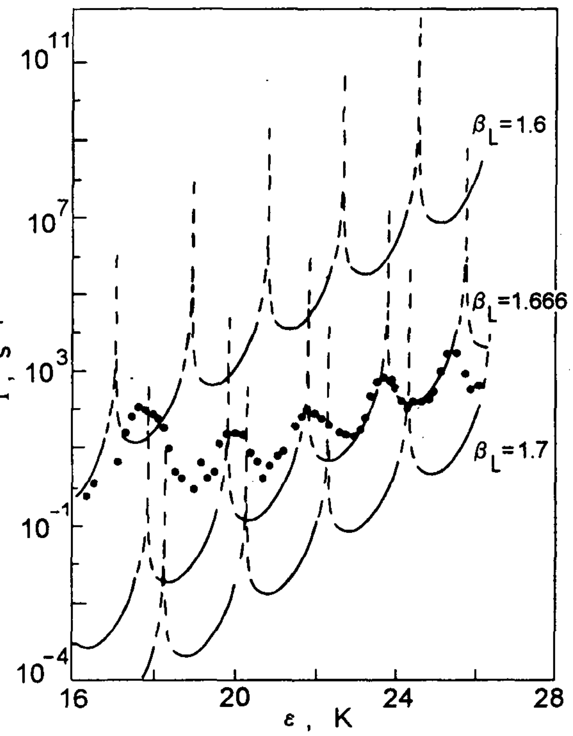

Fig. 12. Calculated escape rate vs potential tilt ε for an rf SQUID, for different β_L values. Here $L = 210$ pH; $C = 80$ fF; $R = 645$ kOhm and $T = 50$ mK, $\beta_L = 1.6655$ corresponds to $\Delta U_0 = 16.3$ K as measured in Ref. 11.

well to the two neighboring levels of the lower well, $E_k^{\rm down}$ and $E_{k+1}^{\rm down}$, where $E_k^{\rm down} < E_0^{\rm up} < E_{k+1}^{\rm down}$. These transition probabilities can be calculated using the same theoretical approach reported in Refs. 32,33, applied for the SQUID potential.

The escape rate from one to another can be calculated according to

$$\Gamma = W_{0,k} - W_{0,k-1} \qquad (13)$$

with

$$W_{0,j} = \frac{E_0^{\rm up} - E_j^{\rm down}}{Re^2}\left(1 + \coth\frac{E_0^{\rm up} - E_j^{\rm down}}{2k_B T}\right)\left|\langle 0|\Phi|j\rangle\right|^2;$$
$$j = k, k-1 \ , \qquad (14)$$

here R is the effective resistance. For bias energy $\varepsilon = E_k^{\rm down} + \delta\varepsilon$ $(\delta\varepsilon/\hbar\omega_1 < 1$; ω_1 is the frequency of the small oscillation in the initial well), the relevant matrix element are given by

$$\left|\langle 0|\Phi|j\rangle\right|^2 = \frac{\pi^3}{2\sqrt{2}}\,\frac{(k+1/2)^{k+1/2}}{\Gamma(k+1)\sin^2(\pi\delta\varepsilon/\hbar\omega_1)} \times$$
$$\times \exp\left(-2\tilde{S}(E_0^{\rm up}, \delta\varepsilon)\right) \ , \qquad (15)$$

$$\left|\langle 0|\Phi|j(j=k-1)\rangle\right|^2 =$$
$$= \frac{\pi}{8\sqrt{2}}\,\frac{(k+1/2)^{k+1/2}}{\Gamma(k-1)(M\omega_1/\hbar)\sin^2(\pi\delta\varepsilon/\hbar\omega_1)} \times$$
$$\times \exp\left(-2\tilde{S}(E_0^{\rm up}, \delta\varepsilon)\right) \ ,$$

where $\Gamma(k) = (k-1)!$ and $\tilde{S}(E) = S(E)/\hbar + E_0^{\rm up}/\hbar\omega_1 + \varepsilon/2\hbar\omega_2$. The action $S(E)$ is taken for an extremal paths under the barrier.

In Fig. 12, we present the results of calculations for the SQUIDs parameters as reported in Fig. 2 of Ref. 11.

Considering the complexity of the experimental contest, the agreement appears to be a resonable because of the absence of any fitting parameters in the straightforward use of the theoretical model. However, the plot of the data and theory shows some discrepancies, mainly in a broadening of the peaks, besides the large discrepancy of the leftmost peak ascribed in Ref. 11 to the occurrence of photon assisted tunneling. These minor discrepancies may be due to resonant tunneling from excited levels, but they must be understood before any definitive conclusion can be drawn.

Conclusions

We have discussed some our data on the thermal induced escape out of the zero-voltage state of a Josephson junction removing the main assumption of the resistively shunted junction model. We have in fact included in the analysis the voltage dependent dissipation due to quasiparticle tunneling. This dissipation can be seen as given by an effective ohmic resistance $R_{\rm eff}$, which comes out to be related, within our model, to a subgap resistance measured on the I–V characteristics, although substantially smaller. At temperatures below $T = 2.8$ K, the effective resistance $R_{\rm eff}$ has been experimentally determined by fitting the current switching distributions. $R_{\rm eff}$ shows the typical exponential temperature dependence due to the presence of quasi-particles thermally activated above the superconducting gap Δ. This circumstance clearly shows that $R_{\rm eff}$ is dominated by an intrinsic quasiparticle mechanism as are the other subgap resistances. The very good agreement of the data with theory confirms the correctness of our assumptions as well as the possibility of a simple determination of the effective resistance from the dc current-voltage curves of the junction. We have clearly shown the relevance of the quasiparticle current in the junction damping, and this intrinsic mechanism dominates, in our experimental configuration, up to rather high resistance values.

The extremely low dissipation level which can be obtained in this way, allows us to study a new effect related to the quantum behavior in the presence of dissipation. We have shown that a fast sweep of the current biasing the junction, which in turn induces nonstationary conditions in the escape process, can modify the shape of the current switching distribution $P(I)$, which becomes an oscillating function of the current. The effect which is very large without the need for microwave irradiation, is due to the presence of discrete energy levels in the potential well. We have then investigated the dependence, under nonstationary conditions, of the current switching distributions both on the temperature and on the dissipation level. As a peculiar aspect of this behavior, we stress that the effect of the energy levels discreteness becomes evident at temperatures larger than the crossover temperature, and it is greater for decreasing damping values. The curves shown predict the results of new possible experiments. Experimental effort in this direction is in progress.

Finally, using as starting point the work by Larkin, Ovchinnikov and Schmidt [32,33], we have shown that the possibility of a resonant macroscopic quantum tunneling produced sharp voltage peaks in the I–V characteristic of a Josephson junction. The new effect is interesting by itself and also in view of possible applications. From an experimental point of view, it requires larger junction areas with respect to experiments on Coulomb blockade, reducing the technological difficulties in making the samples. Our approach allows us to include the temperature explicitly in the calculations, both for what concerns the resonant tunnel probability γ_0 and for escape rate to the free running state. Our results, extrapolated to $T = 0$, are in a reasonable agreement with those of Ref. 23, confirming the great difficulties one would find in trying to reveal the voltage steps. This is due to a small lifetime for voltages large enough to be measured. The phenomenon also produces (for current corresponding to the resonant conditions in the well) sharp peaks in the escape rate to the running state. These peculiar peaks seem, at the moment, the most readily observable effect due to RMQT in current-biased Josephson junctions. Very recently an important experimental result [11], referring to a SQUID rather than to a single junction structure, clearly has shown the occurrence of RMQT in a macroscopic system. The dynamic of the SQUID may be simpler since after each tunneling event a different observable state is reached, while in a single current-biased junction this is obtained only after a sequence of tunneling events. The positions of the maxima agree well with the calculated level crossing and therefore the experiment has been interpreted as due to quantum effects.

We have presented the first theoretical plot for the effect observed.

Considering the complexity of the experimental contest, the agreement appears to be resonable since the absence of any fitting parameters in the straightforward use of the theoretical model. However, the plot of the experimental data and theory shows some discrepancies, mainly in a broadening of the peaks, in addition, there is the large discrepancy of the leftmost peak which ascribed by the authors of Ref. 11 to the occurrence of photon assisted tunneling.

Acknowledgments

The authors are grateful to Antonio Barone for useful discussion and suggestions. This work is partially supported by the Consiglio Nazionale delle Ricerche under the Progetto Finalizzato «Superconductive and Cryogenic Technologies».

1. A. D. Caldeira and A. J. Leggett, *Phys. Rev. Lett.* **46**, 211 (1981). See also A. J. Leggett, in: *Quantum Tunneling in Condensed Media*, Yu. Kagan and A. J. Leggett (eds.), Elsevier Science Pub. (1992), 2 and references therein.
2. A. I. Larkin and Yu. N. Ovchinnikov, *Zh. Eksp. Teor. Fiz.* **91**, 318 (1986) [*Sov. Phys. JETP* **64**, 185 (1986)].
3. C. D. Tesche, *Phys. Rev. Lett.* **64**, 2358 (1990).
4. K. K. Likharev and A. B. Zorin, *J. Low Temp. Phys.* **59**, 347 (1985). For experiments on the subject, see L. J. Geerligs, M. Peters, L. M. de Groot, A. Verbruggen, and J. E Mooij, *Phys. Rev. Lett.* **63**, 326 (1989) and L. J. Geerligs, V. F. Anderegg, J. Romijn, and J. E. Mooij, *Phys. Rev. Lett.* **65**, 377 (1990).
5. D. V. Averin and K. K. Likharev, *J. Low Temp. Phys.* **62**, 345 (1986).
6. S. Washburn, R. F. Voss, R. A. Webb, and S. Faris, *Phys. Rev. Lett.* **54**, 2712 (1985).
7. D. B. Schwartz, B. Sen, C. N. Archie, and J. Lukens, *Phys. Rev. Lett.* **57**, 1547 (1985).
8. M. H. Devoret, J. M. Martinis, D. Esteve, and J. Clarke, *Phys. Rev. Lett.* **53**, 1260 (1984).
9. J. M. Martinis, M. H. Devoret, and J. Clarke, *Phys. Rev. Lett.* **55**, 1543, (1985); M. H. Devoret, J. M. Martinis, and J. Clarke, *Phys. Rev. Lett.* **55**, 1908 (1985); J. M. Martinis, M. H. Devoret, and J. Clarke, *Phys. Rev.* **B35**, 4682 (1987) and references therein.
10. D. Esteve, M. H. Devoret, and J. M. Martinis, *Phys. Rev.* **B34**, 158 (1986).
11. R. Rouse, Siyuan Han, and J. E. Lukens, *Phys. Rev. Lett.* **75**, 1614 (1995).
12. A. Barone and G. Paterno, in: *Physics and Applications of Josephson Effect*, Wiley Pub., New York (1982), Ch. 6.
13. P. Silvestrini, O. Liengme, and K. E. Gray, *Phys. Rev.* **B37**, 1525 (1988); P. Silvestrini, R. Cristiano, S. Pagano, O. Liengme, and K. E. Gray, *Phys. Rev. Lett.* **60**, 844 (1988).
14. J. R. Kirtley, C. D. Tesche, W. J. Gallagher, A. W. Kleinsasser, R. L. Sandstrom, and S. I. Raider, *Phys. Rev. Lett.* **61**, 2372 (1988).
15. P. Silvestrini, *Phys. Rev.* **B46**, 5470 (1992).
16. P. Silvestrini, *Phys. Rev. Lett.* **63**, 211 (1989). See also P. Silvestrini, *Il Nuovo Cimento* **D11**, 897 (1989) and P. Silvestrini and B. Ruggiero, *Il Nuovo Cimento* **D14**, 451 (1992).
17. H. A. Kramers, *Physica* **7**, 284 (1940).
18. M. Buttiker, E. P. Harris, and R. Landauer, *Phys. Rev.* **B28**, 1268 (1983) and references therein.
19. P. Silvestrini and B. Ruggiero, *Il Nuovo Cimento* **D14**, 555 (1992).

20. B. Ruggiero and P. Silvestrini, *Fiz. Nizk. Temp.* **20**, 234 (1994) [*Low Temp. Phys.* 20, 307 (1994)].
21. P. Silvestrini, Yu. N. Ovchinnikov, and R. Cristiano, *Phys. Rev.* B41, 7341 (1990).
22. P. Silvestrini, *Phys. Lett.* A152, 306 (1991).
23. J. M. Schmidt, A. N. Clealand, and J. Clarke, *Phys. Rev.* **B43**, 229 (1991).
24. N. Hatakenaka, S. Kurihara, and H. Takayanagi, *Phys. Rev.* B42, 3987 (1990).
25. A. V. Zhuravlev and A. B. Zorin, *Sov. J. Low Temp. Phys.* **16**, 102 (1990).
26. Yu. N. Ovchinnikov, P. Silvestrini, B. Ruggiero, and A. Barone, *J. Supercond.* 5, 481 (1992).
27. P. Silvestrini and B. Ruggiero, *IEEE Trans. on Supercond.* 5, 3081 (1995); Yu. N. Ovchinnikov, P. Silvestrini, B. Ruggiero, A. Esposito, and A. Barone, *Phys. Rev.* B (in press).
28. For detailes see Ref. 15.
29. The details of the technique to fit the data are extensively discussed in: P. Silvestrini, O. Liengme, and K. E. Gray, *Phys. Rev.* B37, 1525 (1988).
30. Yu. N. Ovchinnikov and B. Ivlev, *Phys. Rev.* B39, 9000 (1989).
31. P. Kopietz and S. Chakravarty, *Phys Rev.* B38, 97 (1988).
32. A. I. Larkin, Yu. N. Ovchinnikov, and A. Schmid, *Physica* B152, 266 (1988).
33. Yu. N. Ovchinnikov and A. Schmid, *Phys Rev.* B50, 6332(1994).